

Flat band in superconducting layers of 2H-TaSe₂

J.A. Galvis,¹ P. Rodière,² I. Guillamon,^{1,3} M.R. Osorio,¹ J.G. Rodrigo,¹
L. Cario,⁴ E. Navarro-Moratalla,⁵ E. Coronado,⁵ S. Vieira,¹ and H. Suderow*¹

¹*Laboratorio de Bajas Temperaturas, Departamento de Física de la Materia Condensada
Instituto de Ciencia de Materiales Nicolás Cabrera, Facultad de Ciencias
Universidad Autónoma de Madrid, E-28049 Madrid, Spain*

²*Institut Néel, CRS/UJF, 25, Av. des Martyrs, BP166, 38042 Grenoble Cedex 9, France*

³*H.H. Wills Physics Laboratory, University of Bristol, Tyndall Avenue, Bristol, BS8 1TL, UK*

⁴*Institut des Matériaux Jean Rouxel (IMN), Université de Nantes, CNRS,
2 rue de la Houssinière, BP 32229, 44322 Nantes Cedex 03, France*

⁵*Instituto de Ciencia Molecular (ICMol), Universidad de Valencia,
Catedrático José Beltrán 2, 46980 Paterna, Spain*

We report scanning tunneling spectroscopy measurements at 150 mK in single layer crystals of 2H-TaSe₂. We find a singular spatial dependence of the tunneling conductance, changing from a zero bias peak on top of Se atoms to a gap in between Se atoms. The zero bias peak is additionally modulated by the commensurate $3a_0 \times 3a_0$ charge density wave of 2H-TaSe₂. Multilayers of 2H-TaSe₂ show, by contrast, a homogeneous superconducting gap with a critical temperature of about 1 K. The zero bias peak in single layers of 2H-TaSe₂ evidences a zero energy bound state. We discuss possible origins for such a peculiar electronic spectrum, which seems to be characteristic of small superconducting single layers of 2H-TaSe₂.

Single layer crystals of dichalcogenide materials can be obtained through repeated exfoliation[1–3]. In spite of extensive searches, no clear experimental evidence of superconductivity has been found in them. On the other hand, in-situ grown single layer surfaces, mostly of Pb, are creating a rich playground, demonstrating that superconductivity can form in atomically thin crystals. However, the superconducting critical temperature T_c decreases when achieving ultimate thickness[4–6], and the superconducting tunneling conductance shows s-wave BCS like gap features[7]. Signs of unconventional superconductivity, as proposed in doped graphene layers[8, 9], are until now absent.

TaSe₂ is a transition metal dichalcogenide, which crystallizes in a layered structure with small interlayer coupling. The layers are made of Se-Ta-Se units with two triangular sheets of Se atoms separated by one sheet of Ta atoms. Interlayer bonding is weak through van der Waals forces. The relative arrangement of the Se triangles varies in different polytypes of the same compound. Of interest here are the 2H and the 1T polytypes. 2H has a unit cell consisting of two TaSe₂ units, each built up by two Se triangles separated by Ta atoms. The unit cell of the 1T polytype is composed of a single layer of TaSe₂, with the Se triangles rotated to each other by 30°[10]. 2H polytypes of similar compounds such as 2H-NbSe₂ and 2H-TaS₂ have been subject of much discussion regarding the coexistence of superconductivity with a charge density wave (CDW) [11–14]. The c-axis interlayer coupling decreases from 2H-NbSe₂, 2H-TaS₂ to 2H-TaSe₂. Superconductivity in 2H-NbSe₂ is s-wave, with a strong in-plane anisotropy related to the charge density wave, and in 2H-TaS₂ it emerges out of a chiral electronic charge density wave[13–15]. There are few reports

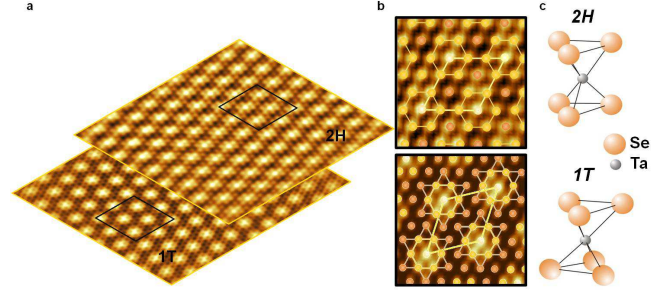


FIG. 1: We show a schematic representation of the atomic arrangements discussed. We highlight the top sheet as 2H. It shows a $3a_0 \times 3a_0$ superlattice modulated charge density wave (CDW). The layer immediately below, highlighted as 1T has a different Moiré pattern with a $\sqrt{13}a_0 \times \sqrt{13}a_0$ CDW. In 2H-TaSe₂, top and bottom Se atoms are aligned (top figure in c). In 1T-TaSe₂, the two Se triangles are rotated (bottom figure in c). The middle panels (b) show in more detail the CDW patterns found in each area. There are three inequivalent atomic sites in the pattern, as highlighted by yellow, orange and white points. The incommensurate CDW $\sqrt{13}a_0 \times \sqrt{13}a_0$ pattern shown in the bottom panel of (b) consists of stars of David, with also three inequivalent sites. The arrangement shown in (a), with one 2H-TaSe₂ sheet on top 1T-TaSe₂ presents the singular superconducting features discussed in the following figures.

about superconductivity in 2H-TaSe₂, showing superconducting diamagnetic signals and zero resistance at temperatures below 150 mK [10, 16, 17], as compared to 2H-TaS₂ ($T_c=0.8$ K) and 2H-NbSe₂ ($T_c=7$ K). Charge order in 2H-TaSe₂ is incommensurate between 122 K and 90 K, below which it locks into a $3a_0 \times 3a_0$ (with a_0 being the in plane lattice parameter) commensurate charge modulation[18, 19]. 1T-TaSe₂ also develops a charge den-

sity wave at low temperatures[10, 20], with, however, a periodicity of $\sqrt{13}a_0 \times \sqrt{13}a_0$ rotated by 13.5° with respect to the atomic lattice[18, 21]. Within the charge ordered state, 1T-TaSe₂ is a so-called "bad metal" with a high in-plane resistivity and a c-axis mean free path below the interplanar distance. No superconductivity has been reported in this material so far at ambient pressure and without doping. One of the most direct methods to determine the polytype of the surface is to measure the charge modulations using Scanning Tunneling Microscopy (STM). Here we study 2H-TaSe₂ using scanning tunneling spectroscopy at 150 mK and demonstrate that repeated exfoliation gives surfaces with single layer crystals of 2H-TaSe₂ on top of 1T-TaSe₂. The single layer crystals of 2H-TaSe₂ have radically different properties than the bulk, with peculiar tunneling features varying at atomic sizes.

We measure TaSe₂ in a STM system installed in a dilution refrigerator that can reach temperatures down to about 150mK. The STM has a sample holder that allows us to change *in-situ* the scanning window[22]. We use a tip prepared from a gold wire cut with a clean blade. The residual resistivity ratio of the TaSe₂ samples is of 26, implying samples similar to those used to observe quantum oscillations and measure the Fermi surface[23–25]. Bulk susceptibility measurements of our samples give a diamagnetic signal with the same T_c as in previous work (150 mK)[10, 16, 17]. Samples are freshly cleaved before inserting them into the set-up, and we take atomic resolution topographic images at a constant tunneling current, and bias voltages below 2 mV, with tunneling conductance of the order of some $0.1 \mu\text{S}$.

The STM topography shows the atomic Se lattice and either the $3a_0 \times 3a_0$ CDW with the same orientation to the Se lattice and commensurate to it, or Moiré patterns characteristic of a CDW with a periodicity of $\sqrt{13}a_0 \times \sqrt{13}a_0$ rotated by 13.5° with respect to the atomic Se lattice. The first identifies 2H-TaSe₂ surfaces, and the second 1T-TaSe₂ surfaces (Fig.1). We find atomically flat 2H-TaSe₂ layers, between 50 nm to 300 nm in lateral size, showing immediately below a surface of 1T-TaSe₂. Steps between both surfaces are of 1.2 nm, corresponding to two layers of the sandwich Se-Ta-Se. Thus, the upper layers are single layer crystals of 2H-TaSe₂. We also find 1T-TaSe₂ or 2H-TaSe₂ surfaces over large areas and many different steps. These correspond to multilayer 1T-TaSe₂, and 2H-TaSe₂, respectively.

We have made a thorough spectroscopy and microscopy characterization of all observed surfaces by taking simultaneously topography and tunneling conductance (Fig.2). In left panels of Fig.2a we show curves obtained when scanning from the top of a Se atom to an intersite at the center of three Se atoms. On single layer crystals of 2H-TaSe₂, a clear zero bias peak is observed on top of the Se atom. The zero bias peak evolves continuously into a V-shape conductance at the intersite

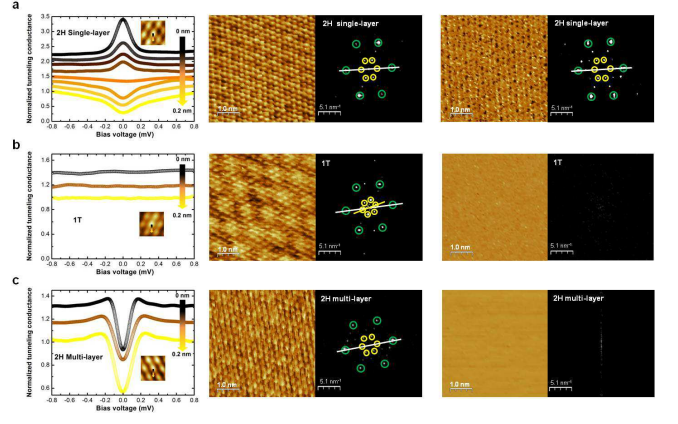


FIG. 2: Tunneling conductance versus bias voltage in single layer 2H-TaSe₂ (a), in 1T-TaSe₂ (b) and in multilayer 2H-TaSe₂ (c). Tunneling conductance curves in left panels are taken when the tip moves from a Se atom (black) to an intersite (yellow). Insets show relevant atomic size topography images. Larger scale topography (z scale around 0.5 nm) and the corresponding Fourier transforms are shown in middle panels. Green circles show the position of the Bragg peaks due to the atomic Se modulation and yellow circles show the peaks due to the CDW modulation. Lines are shown to highlight the angular difference between atomic and CDW modulations. The zero bias conductance maps show contrast in single layer 2H-TaSe₂ a, where black points correspond to curves similar to the black tunneling conductance curve shown in the left panel, and yellow points to yellow tunneling conductance curves. The two other conductance maps have a color scale corresponding to a change of 0.1 in normalized conductance units, showing thus that they are fully flat. All images shown here are unfiltered.

between three Se atoms. In 1T-TaSe₂ layers (Fig.2b), we find featureless metallic flat tunneling conductance curves. In multilayers of 2H-TaSe₂ (Fig.2c), the superconducting gap opens with a size of the order of $150 \mu\text{V}$ and quasiparticle peaks that do not change as a function of the position over the surface.

The zero bias tunneling conductance map of single layer crystals of 2H-TaSe₂ (right panel of Fig.2a) mimics the topography. However, in 1T-TaSe₂ (right panel of Fig.2b) and in 2H-TaSe₂ multilayers (right panel of Fig.2c), conductance maps are flat and featureless. In Fig.3 we show other representative examples of single layers of 2H-TaSe₂. The features in the conductance maps smoothly disappear when the bias voltage is increased above approximately $300 \mu\text{eV}$, where the tunneling curves become flat.

More detailed real space imaging of the 2H-TaSe₂ single layer is shown in Fig.4. The atomic and CDW modulations are observed simultaneously on the zero bias conductance map and the topography. In particular, the Fourier transform image of the zero bias conductance map shows the atomic Se lattice and the CDW. In real space, we observe that the highest value for the zero bias

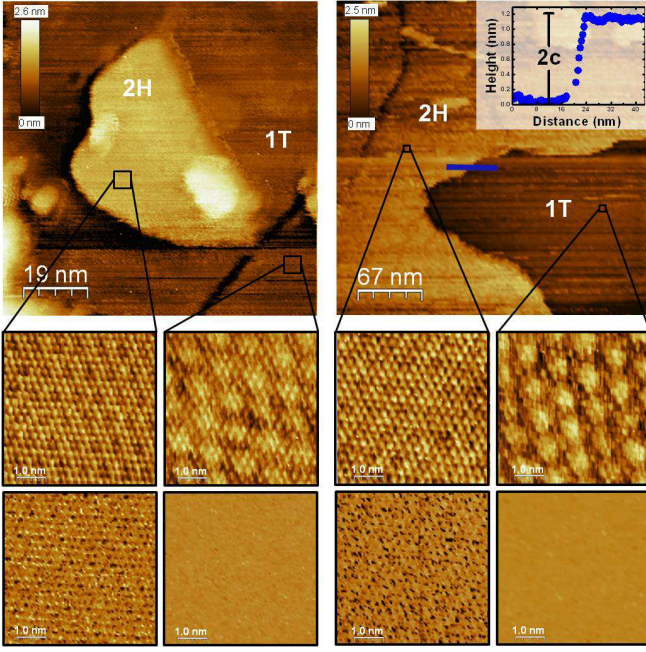


FIG. 3: Large topographic images in the top panels, and zoom-ups of different areas in the middle panels. The bottom panels are conductance maps taken at zero bias in the same areas as the small size topographic images shown in the middle panels. In all cases we observe a 2H-TaSe₂ single layer on top of 1T-TaSe₂. The hexagonal layer shows the features in the conductance discussed in Fig.2a, and the trigonal layer is featureless. Images here are unfiltered and have been taken at 0.15 K. Height profiles across steps between 2H and 1T surfaces have a size of the order of a single 2H-TaSe₂ layer ($2c = 1.2\text{nm}$).

quasiparticle peak (blue curve in Fig.4b) coincides with the brightest Se atom due to the CDW (white points in Fig.4a). On the other hand, the V-shape gap (yellow curves in Fig.2a and in Fig.4b) between Se atoms is homogeneous.

Measurements of these features as a function of the temperature and magnetic field show that the zero bias peak and the V-shaped conductance in single layers as well as the superconducting gap observed in multilayers (Fig.2c) disappear at a temperature of 1 K. The weak coupling superconducting gap equation $\Delta = 1.76k_B T_c$ gives, for $T_c = 1\text{ K}$, $150\mu\text{eV}$, which coincides with the width of the V-shape and the zero bias peak in the hexagonal layer (Fig.2a and Fig.4b), as well as the size of the superconducting gap in multilayers (Fig.2c). Application of a magnetic field perpendicular to the sample surface leads flat featureless curves at a very low field, below 100 mT. Thus we conclude that the zero bias peak of the single layer (Fig.2a) and the clear gap with quasiparticle peaks of the multilayers (Fig.2c) are both evidencing superconducting properties of single and multilayer 2H-TaSe₂.

Our curves do not change qualitatively when approach-

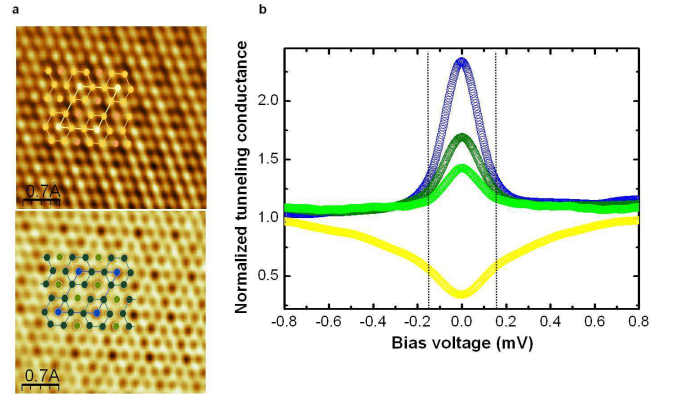


FIG. 4: Topography (top panel) and tunneling conductance map at zero bias (bottom panel) of a hexagonal layer on top of a trigonal layer. Images, taken at 0.15 K, are filtered for clarity. The blue, dark and light green curves of b are taken all three on top of Se atoms, corresponding to the color code shown in the bottom panel of a. The yellow curve is taken in between Se atoms. The curves on top of the Se atoms all show a zero bias conductance peak, whose height is modulated as a function of the position. Blue curves are located at the Se position which also shows highest contrast in the topography (white on top panel of a). Dark green and light green curves are located at the other Se positions with different charge modulations. Yellow curve is independent of the position in the CDW modulation.

ing the steps separating layers. The tunneling features of 1T-TaSe₂ are homogeneous and metallic like up to the step to a layer of 2H-TaSe₂. Thus, there are no classical superconducting proximity effects induced among layers showing different properties, pointing to significant electronic de-coupling. The single layers of 2H-TaSe₂ give a low dimensional superconductor electronically decoupled from its substrate, which is actually formed by the same material crystallizing in another polytype.

The presence of single layer crystals of 2H-TaSe₂ on top of non-superconducting 1T-TaSe₂ is often found on the surface of freshly cleaved samples of 2H-TaSe₂. We have characterized several 2H-TaSe₂ single layer crystals obtained in different samples, finding the intricate hexagonal pattern in the spectroscopy on single layer crystals of 2H-TaSe₂.

The zero bias conductance peak on top of the Se atoms evidences a very large density of states at zero energy. Large or diverging densities of states indicate the presence of a flat band, appearing in this case at the Fermi level. The variations in the height of the zero bias peak with the CDW (Fig.4b) is an additional feature showing the involvement of charge order in shaping the changes in the superconducting properties responsible for the creation of the zero energy state. These variations also show the extreme position dependence of the observed features, with the zero bias peak changing into a V-shaped gap nearly at subatomic sizes. Atomic

size changes in the superconducting tunneling conductance have been observed previously due to the in-plane anisotropic gap structure of 2H-NbSe₂, and are the result of the tip probing different parts of the band structure, due to differing tip-sample coupling as a function of the atomic site[26, 27]. Note that 2H-TaSe₂ has two rather wide bands derived from Ta d electrons crossing the Fermi level, and the coherence length is large (around 500 nm[19, 28, 29]), above the lateral size of the single layers. Thus, perturbations of superconductivity will extend rather homogeneously over the whole layer. This, together with the atomic size dependence of the tunneling features, shows that the single layers of 2H-TaSe₂ have a very intricate band structure, with a Fermi level state and the concomitant flat band, coexisting with a V-shaped electronic density of states.

Resonant bound states leading to flat bands close to the Fermi level are found e.g. at the core of magnetic vortices in clean superconductors, because of multiple Andreev reflection[30]. The first state is not located at zero energy, but at Δ^2/E_F , which is generally small but finite. At zero magnetic field, in-gap bound states also arise at magnetic impurities in s-wave superconductors [31–33]. Their energy location depends on the relative amplitude of electron and hole impurity wavefunctions, which is governed by the exchange interaction between the localized magnetic moments of the impurity and the Cooper pairs, or by the scattering phase shift[32]. When scattering is resonant, the impurity bound state occurs exactly at the Fermi level, and the impurity spin is screened by an in-gap state oppositely polarized, in a similar way to Kondo screening in a normal metal through singlet formation[32]. On the other hand, zero energy resonant bound states located exactly at the Fermi level arise naturally in reduced symmetry superconductors, such as d-wave or more complex superconductors, when some kind of scattering leads to a sign change or a phase slip of the underlying wavefunction. A zero voltage conductance peak can appear thus close to impurities, at a surface or close to crystal boundaries [8, 32, 34–39]. Thus, to obtain a zero voltage peak over whole single layer flakes, we need either resonantly scattering magnetic impurities, for which we find no indications, or unconventional superconductivity together with some strong scatterer such as the border, defects or the surface. The latter suggestion is intriguing, and would imply that the superconducting properties change from conventional s-wave in multilayers to unconventional reduced symmetry superconductivity when decreasing the thickness of the sample down to a single layer.

The electronic structure of multilayers and the single layer is very similar, as shown by the charge density wave which remains the same as in the bulk. However, the superconducting properties are clearly modified. We can speculate that charge order is more effective in building complex shapes of the superconducting wavefunction in

single layers. Evidences for charge order shaped superconducting properties have been obtained in bulk measurements in 2H-NbSe₂[26]. It remains to be seen if the single layer case is an extreme case of charge order shaped superconductor, or an unexpected effect of reduced size and dimensionality.

Another intriguing finding is of course the increase of the critical temperature with respect to bulk 2H-TaSe₂. The critical temperature of these materials is easy to enhance through pressure or strain[20, 28, 40, 41], so that the increase of T_c maybe just a surface effect, absent in other dichalcogenides where the bulk T_c is higher and closer to the maximum T_c obtained in these materials[40].

In summary, we have found highly anomalous tunneling conductance features in single layer 2H-TaSe₂ obtained through exfoliation on crystals of the same compound. We observe a zero bias peak extended over whole single layer crystals of 2H-TaSe₂ when they lie on top of a surface of 1T-TaSe₂. The zero bias peak is modulated by a charge density wave, and coexists with a V-shaped gap feature. Important questions arise from our data: what is the role of the stacking with different polytypes in the interplay between superconductivity and charge order? and how do properties change when stacking two, three or more layers of 2H-TaSe₂? Further study of this and other dichalcogenides could unveil a new class of materials where single layer properties lead to superconducting features totally different from bulk materials.

We acknowledge discussions with F. Guinea, V. Vinokur, T. Baturina, A.I. Buzdin and P. Monceau. We also acknowledge advice and discussions about the dichalcogenides with J.L. Vicent. The Laboratorio de Bajas Temperaturas is associated to the ICMN of the CSIC. This work was supported by the Spanish MINECO (Consolider Ingenio Molecular Nanoscience CSD2007-00010 program, FIS2011-23488, MAT2011-25046 and ACI-2009-0905) and by the Comunidad de Madrid through program Nanobiomagnet.

* hermann.suderow@uam.es.

-
- [1] K. Novoselov, D. Jiang, F. Schedin, T. Booth, V. Khotkevich, S. Morozov, and A. Geim, *Proc. Natl. Acad. Sci. USA* **102**, 10451 (2005).
 - [2] K. Novoselov, A. Geim, S. Morozov, D. Jiang, M. Katsnelson, I. Grigorieva, S. Dubonos, and A. Firsov, *Nature* **438**, 197 (2005).
 - [3] A. Castellanos-Gomez, N. Agrait, and G. Rubio-Bollinger, *Applied Physics Letters* **96**, 213116 (2010).
 - [4] S. Qin, J. Kim, Q. Niu, and C.-K. Shih, *Science* **324**, 1314 (2009).
 - [5] T. Cren, D. Fokin, F. Debontridder, V. Dubost, and D. Roditchev, *Phys Rev Lett* **102**, 127005 (2009).
 - [6] T. Zhang, P. Cheng, W.-J. Li, Y.-J. Sun, G. Wuang, X.-G. Zhy, K. He, L. Wang, X. Ma, X. Chen, et al., *Nature*

- Physics **6**, 104 (2010).
- [7] D. Liu and et al., Nature Communications **3**, 931 (2012).
 - [8] R. Nandkishore, L. Levitov, and A. Chubukov, Nature Physics **8**, 158 (2012).
 - [9] G. Profeta, M. Calandra, and F. Mauri, Nature Physics **8**, 131 (2012).
 - [10] J. A. Wilson, F. J. DiSalvo, and S. Mahajan, Adv. Phys. **24**, 117 (1975).
 - [11] W. Sacks, D. Roditchev, and J. Klein, Phys. Rev. B **57**, 13118 (1998).
 - [12] A. H. Castro Neto, Phys. Rev. Lett. **86**, 4382 (2001).
 - [13] I. Guillamon, H. Suderow, J. Rodrigo, S. Vieira, P. Rodiere, L. Cario, E. Navarro-Moratalla, C. Marti-Gastaldo, and E. Coronado, New J. of Phys. **13**, 103020 (2011).
 - [14] J. van Wezel, Phys. Rev. B **85**, 035131 (2012).
 - [15] J. Ishioka, Y. Liu, K. Shimatake, T. Kurosawa, K. Ichimura, Y. Toda, M. Oda, and S. Tanda, Phys. Rev. Lett. **105**, 176401 (2010).
 - [16] T. Kumakura, H. Tan, T. Handa, M. Morisita, and H. Fukuyama, Czechoslovak Journal of Physics **46**, 261 (1996).
 - [17] K. Yokota, G. Kurata, T. Matsui, and H. Fukuyama, Physica B **284-288**, 551 (2000).
 - [18] C. Slough, W. McNairy, R. Coleman, B. Drake, and P. K. Hansma, Phys. Rev. B **34**, 994 (1986).
 - [19] K. Rossnagel, J. Phys. Cond. Matt. **23**, 213001 (2011).
 - [20] L. Bulaevskii, Sov. Phys. Usp. **19**, 836 (1976).
 - [21] B. Giambattista, A. Johnson, R. Coleman, B. Drake, and P. K. Hansma, Phys. Rev. B **37**, 2741 (1988).
 - [22] H. Suderow, I. Guillamon, and S. Vieira, Rev. Sci. Inst. **82**, 033711 (2011).
 - [23] S. Hillenius and R. Coleman, Phys. Rev. B **18**, 3790 (1978).
 - [24] R. Fleming and R. Coleman, Phys. Rev. B **16**, 302 (1977).
 - [25] J. Graebner and M. Robbins, Phys. Rev. Lett. **36**, 422 (1976).
 - [26] I. Guillamón, H. Suderow, F. Guinea, and S. Vieira, Phys. Rev. B **77**, 134505 (2008).
 - [27] J. E. Hoffman, E. W. Hudson, K. M. Lang, and et al., Science **295**, 466 (2002).
 - [28] D. E. Moncton, J. D. Axe, and F. J. DiSalvo, Phys. Rev. B **16**, 801 (1977).
 - [29] S. Borisenko, A. Kordyuk, A. Yaresko, V. Zabolotny, D. Inosov, R. Schuster, B. Buchner, R. Weber, R. Follath, L. Patthar, et al., Phys. Rev. Lett. **100**, 196402 (2008).
 - [30] C. Caroli, P. G. de Gennes, and J. Matricon, Phys. Lett. **9**, 307 (1964).
 - [31] A. Yazdani, B. A. Jones, C. P. Lutz, M. F. Crommie, and D. M. Eigler, Science **275**, 1767 (1997).
 - [32] A. V. Balatsky, I. Vekhter, and J.-X. Zhu, Rev. Mod. Phys. **78**, 373 (2006).
 - [33] K. Franke, G. Shulze, and J. Pascual, Science **332**, 940 (2012).
 - [34] Y. Tanaka and S. Kashiwaya, Phys. Rev. B **53**, 9371 (1996).
 - [35] S. Pan, E. Hudson, K. M. Lang, H. Eisaki, S. Uchida, and J. C. Davis, Nature **403**, 746 (2000).
 - [36] G. Volovik, JETP Lett. **93**, 66 (2011).
 - [37] A. Schnyder and S. Ryu, Phys. Rev. B **84**, 060504(R) (2011).
 - [38] C. Stephanos, T. Kopp, J. Mannhart, and P. Hirschfeld, Phys. Rev. B **84**, 100510(R) (2011).
 - [39] N. Kopnin, T. Heikkila, and G. Volovik, Phys. Rev. B **83**, 220503(R) (2011).
 - [40] H. Suderow, V. Tissen, J. Brison, J. Martinez, and S. Vieira, Phys. Rev. Lett. **95**, 117006 (2005).
 - [41] E. Coronado, C. Marti-Gastaldo, E. Navarro-Moratalla, A. Ribera, S. Blundell, and P. Bajer, Nature Chemistry **2**, 1031 (2010).